


 Cite this: *CrystEngComm*, 2016, **18**, 3223

Pressure-preferred symmetric reactions of 4,4'-bipyridine hydrobromide[†]

Michalina Anioła and Andrzej Katrusiak*

High pressure and temperature trigger symmetric chemical reactions of 4,4'-bipyridine hydrobromide monohydrate ($44'\text{biPyHBr}\cdot\text{H}_2\text{O}$) in methanol solution. Above 0.1 GPa and 423 K, the 4,4'-bipyridinium dibromide salt ($44'\text{biPy2HBr}$) precipitates, while the 4,4'-bipyridine free base remains dissolved in the methanol–water mixture. At 0.35 GPa and 473 K, both pyridine moieties are *N*-methylated and *N,N*-dimethylbipyridinium dibromide ($44'\text{biPy2CH}_3\text{Br}$) is formed. None of the high-pressure compounds of $44'\text{biPy2HBr}$ and $44'\text{biPy2CH}_3\text{Br}$ are solvated, which contrasts with the strong preference of analogous 1,4-diazabicyclo[2.2.2]octane (dabco) monosalts and disalts to form solvates at high-pressure. The high-pressure reactivity of $44'\text{biPyHBr}$ is analogous to that of 1,4-diazabicyclo[2.2.2]octane hydrobromide (dabcoHBr); however, dabcoHBr is asymmetrically *N*-methylated at one amine site only. This asymmetric mono *N*-methylation of dabcoHBr has been associated with strong electrostatic interactions between the transannular N-atoms.

 Received 11th February 2016,
 Accepted 18th March 2016

DOI: 10.1039/c6ce00356g

www.rsc.org/crystengcomm

Introduction

High-pressure can drastically change the reactivity of chemical compounds and their properties.¹ This knowledge, well-exemplified by deep-crust minerals,² is relatively seldom employed in chemical laboratories. Usually very high-pressure (of tens and hundreds of GPa) is applied for synthesizing super-hard minerals,^{3,4} and a lower range of pressures (few MPa) is used for synthesizing metal–organic frameworks (MOF).⁵ Pressure significantly affects the conformation and interactions of organic molecules, which equally applies to molecular and ionic substrates. Intriguing pressure effects were observed for 1,4-diazabicyclo[2.2.2]octane hydrobromide (dabcoHBr) and hydroiodide (dabcoHI) dissolved in methanol and in water. It was established that pressure and temperature strongly affect the structure of these compounds: ten polymorphs were identified for dabcoHI⁶ and three polymorphs for dabcoHBr.⁷ It was also observed that pressures above 0.5 GPa efficiently promote the solvation of dabcoHI and two polymorphs of monohydrate dabcoHI·H₂O were obtained,⁸ while a pressure of 3.1 GPa is required for obtaining a mixed solvate with water and methanol, dabcoHI·H₂O·CH₃OH.⁹ Treatment of an anhydrous methanol : ethanol dabcoHI solution above 1.4 GPa yielded a solvated disalt, dabco2HI·3CH₃OH,¹⁰ but analogous treatment of dabcoHBr

does not lead to the disalt formation. Both in dabcoHBr and dabcoHI dissolved in methanol, the still higher pressures of 1.8 GPa and 2.4 GPa, respectively, above 350 K promoted the

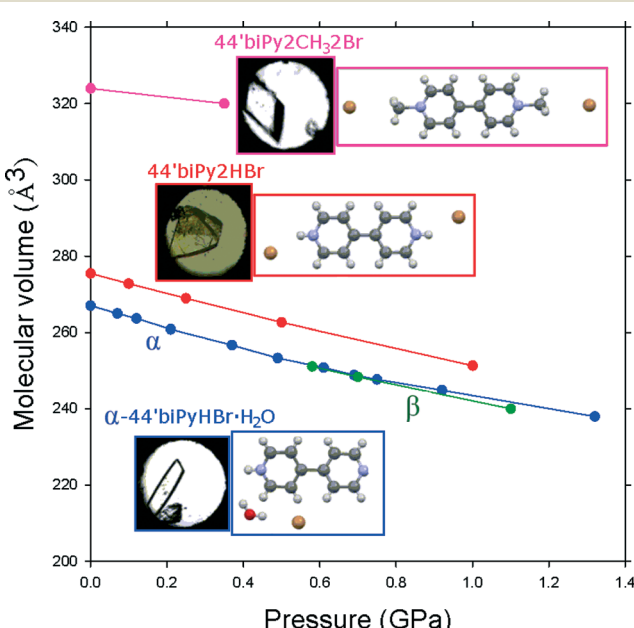


Fig. 1 Molecular volume (V/Z) of 4,4'-bipyridine hydrobromide monohydrate ($44'\text{biPyHBr}\cdot\text{H}_2\text{O}$, phases α and β), 4,4'-bipyridine dihydrobromide ($44'\text{biPy2HBr}$) and *N,N*-dimethyl-4,4'-bipyridine dibromide ($44'\text{biPy2CH}_3\text{Br}$) as a function of pressure. The insets show the crystals in the diamond-anvil cell (DAC) chamber and the structural drawings of the formula units (the colors of frames around photographs and formula correspond to the plotted lines and symbols).

Faculty of Chemistry, Adam Mickiewicz University, Umultowska 89b, 61-614 Poznań, Poland. E-mail: katran@amu.edu.pl

† Electronic supplementary information (ESI) available. CCDC 1452481–1452486. For ESI and crystallographic data in CIF or other electronic format see DOI: 10.1039/c6ce00356g



N-methylation reaction and precipitation of mono-*N*-methylated dimethanol solvates: *N*-methyl-1,4-diazabicyclo[2.2.2]octanium bromide dimethanol and *N*-methyl-1,4-diazabicyclo[2.2.2]octanium iodide dimethanol, $[\text{dabcoCH}_3]^+\text{Br}^- \cdot 2\text{CH}_3\text{OH}$ and $[\text{dabcoCH}_3]^+\text{I}^- \cdot 2\text{CH}_3\text{OH}$, respectively.¹¹ Presently we have investigated the effects of pressure on the reactions of disalt formation and *N*-methylation of 4,4'-bipyridine hydrobromide monohydrate, 44'biPyHBr·H₂O. Monosalt 44'biPyHBr significantly differs from dabcoHBr in the preference for the formation of hydrates: from aqueous solution only anhydrous dabcoHBr precipitates, while exclusively monohydrate 44'biPyHBr·H₂O precipitated from aqueous and methanol:water solutions under normal conditions. It was observed most recently that 44'biPyHBr·H₂O can be compressed to 1.32 GPa at least in its ambient pressure form α , built from chains of $\text{NH}^+ \cdots \text{N}$ bonded 44'biPyH⁺ cations (their disproportionated neutral 44'biPy and dication $[44'\text{biPy}2\text{H}]^+$ are also very likely) and of $\cdots \text{HOH} \cdots \text{Br}^- \cdots$ bonded chains. Its recrystallization above 0.55 GPa leads to a new $\text{NH}^+ \cdots \text{N}$ bonded β form.¹² Although the α and β forms of 44'biPyHBr·H₂O are similar in their structure and lattice dimensions, form α does not spontaneously transform into the β form, but on releasing the pressure, the β form transforms into the α form again (Fig. 1).

4,4'-Bipyridine (44'biPy) is widely used in chemical practice and presently there are more than 7000 compounds with 44'biPy moieties and its derivatives deposited with the Cambridge Structural Database.¹³ In many metal-organic frameworks, 44'biPy serves as a linker and its susceptibility to pressure can be essential for the properties of these compounds. It was shown that forms α and β of 44'biPyHBr·H₂O significantly differ in the conformation of cations, twisted and flat, respectively. The high-pressure effects on diamine cyclic monohydrobromides of 4,4'-bipyridine and dabco have been compared in this study.

Experimental

High-pressure experiments were performed in a Merrill-Bassett diamond-anvil cell (DAC)¹⁴ modified by mounting the anvils directly on steel supports with conical windows.¹⁵ The gasket was made of tungsten foil 0.3 mm thick with a hole 0.4 mm in diameter. The DAC chamber was filled with a saturated methanol solution of 44'biPyHBr·H₂O. For pressure calibration, the ruby-fluorescence method was used^{16,17} and the measurements were performed using a Photon Control spectrometer affording the precision of 0.02 GPa. In the first experiment, pressure was increased till a polycrystalline mass precipitated. Then the sample in the DAC chamber was heated to 423 K when all crystal grains dissolved and subsequently a single crystal was grown at isochoric conditions by slowly cooling the DAC (Fig. 2). The formation of dibromide 44'biPy2HBr is marked by its yellow colour, distinct from colourless monobromide 44'biPyHBr·H₂O. Then the pressure was gradually increased and X-ray diffraction data were obtained at 0.1, 0.2, 0.5 and 1.0 GPa. In the next experiment,

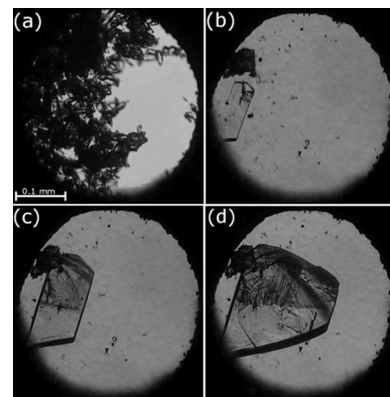


Fig. 2 Crystals precipitated from the saturated methanol solution of 44'biPyHBr·H₂O in the DAC chamber after increasing the pressure to 0.10 GPa (a); a single seed of 44'biPy2HBr obtained after dissolving all the crystals at 423 K and keeping the sample in this temperature for 30 min (b); at 343 K after gradually decreasing the temperature for 60 min (c); and at 0.10 GPa/296 K after 180 min (d). Tiny ruby chips for pressure calibration are grouped at the upper-left edge of the gasket and are scattered in the chamber.

the DAC chamber was filled with the same saturated solution, but the pressure was increased to 0.35 GPa when the isochoric crystallization was started. In order to dissolve all the precipitate at this pressure, the DAC had to be heated to 473 K (Fig. 3). When the DAC was heated to 423 K, the anhydrous disalt 44'biPy2HBr was formed, but a temperature of 473 K triggered the *N*-methylation reaction and the *N,N*-dimethylated disalt 44'biPy2CH₃Br was obtained. All X-ray measurements were performed using a KUMA KM4-CCD diffractometer. The determination of X-ray data and their preliminary reduction were performed with CrysAlis software.¹⁸ Then, the intensities of reflections were corrected for the effects of DAC absorption, sample shadowing by the gasket,

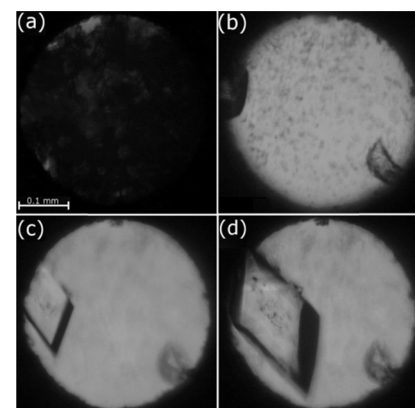


Fig. 3 Crystalline powder precipitated from the saturated methanol solution of 44'biPyHBr·H₂O after increasing the pressure to 0.35 GPa (a); (b) one single-crystal seed of 44'biPy2CH₃Br obtained after 60 min after dissolving the crystals at 473 K; (c) the single crystal at 393 K after gradually reducing the temperature for 90 min; and (d) at 0.35 GPa/296 K after continuing the gradual cooling for 180 min. One ruby chip for pressure calibration lies at the bottom-right edge and several very small ruby grains are scattered in the chamber.



the sample absorption¹⁹ and diamond reflections were eliminated. H-atoms were located from the molecular geometry and isotropic U_{iso} equal to $1.2U_{\text{eq}}$ of the H-carrier was assigned. For the methyl group, the constraints of AFIX 33 were applied in the final model. We have also tried the constraints of AFIX 137, but they resulted in the H-atom positions close to those generated by the AFIX 33 instruction (see Table S1 in the ESI† comparing the two models). The crystallographic and experimental details have been deposited in CIF format with the Cambridge Crystallographic Database Centre as deposits no. CCDC 1452481–1452486.

Discussion

It was previously established that the isothermal or isochoric recrystallizations of 44'biPyHBr·H₂O from methanol solution below 0.55 GPa and 353 K retain the ambient-pressure orthorhombic phase α (space group $P2_{1}2_{1}2_{1}$), while recrystallizations above 0.55 GPa lead to the monoclinic β phase (space group $P2_{1}/c$). Presently we have found that still higher temperatures trigger chemical reactions of 44'biPyHBr·H₂O with methanol. In the chamber loaded with the 44'biPyHBr·H₂O crystals and filled up with its saturated methanol solution, when the pressure was increased to 0.1 GPa, the temperature of 423 K was required to dissolve all the sample. The subsequent slow recrystallization at isochoric conditions resulted in disalt 44,4'-bipyridinium dibromide, 44'biPy2HBr. The precipitation of anhydrous 44'biPy2HBr implies that the following reaction takes place:



The free-base 44'biPy remained dissolved in the methanol : water mixture (the water contents released from the dissolved 44'biPyHBr·H₂O and not absorbed in the precipitate).

The high-pressure structure of anhydrous 44'biPy2HBr is consistent with that of a previously determined triclinic crystal (Table 1).²⁰ In this structure, $\text{NH}^+ \cdots \text{Br}^-$ hydrogen bonds replace the $\text{NH}^+ \cdots \text{N}$ bonds, present in all monoprotonated 44'biPyHA structures (Fig. 4). This feature of the above reaction resembles the pressure-induced solid-state transformations in dabcoHBr, where the $\text{NH}^+ \cdots \text{N}$ bonded chains of the dabcoH⁺ cations present in phase II are replaced by $\text{NH}^+ \cdots \text{Br}^-$ bonded ionic pairs above 0.4 GPa/296 K (in phase III) and at ambient-pressure above 444 K (in phase I).^{7,21} However, the H-bonds transforming in dabcoHBr do not change the mono salt stoichiometry.

Moreover, dabcoHBr could not be transformed into disalt dabco2HBr by applying pressure to about 1.5 GPa and temperature to about 430 K. However, such a pressure-induced disalt formation, analogous to 44'biPy2HBr, was observed in dabco hydroiodide (dabcoHI). At 1.80 GPa, dabcoHI transforms into dabco2HI·3CH₃OH with $\text{NH} \cdots \text{O}$ hydrogen bonds linking the dications with the methanol molecules.¹⁰ On the other hand, both dabcoHBr and dabcoHI, when dissolved in methanol, compressed to 1.2 and 2.4 GPa and heated,

Table 1 Selected crystal data of 44'biPy2HBr at 0.20 GPa/296 K and 44'biPy2CH₃Br at 0.35 GPa/296 K. The full crystallographic data for 44'biPy2HBr at 0.1 MPa, 0.1 GPa, 0.2 GPa, 0.5 GPa and 1.0 GPa, as well as those for 44'biPy2CH₃Br at 0.35 GPa, are listed in Tables S2 and S3 in the ESI

	44'biPy2HBr	44'biPy2CH ₃ Br
<i>p</i> /GPa	0.20 GPa	0.35 GPa
<i>T</i> /K	296	296
Crystal system	Triclinic	Monoclinic
Space group	<i>P</i> 1	<i>P</i> 2 ₁ /c
<i>a</i> /Å	4.874(4)	5.947(3)
<i>b</i> /Å	7.567(6)	8.068(8)
<i>c</i> /Å	7.936(4)	13.411(5)
$\alpha/^\circ$	70.73(6)	90
$\beta/^\circ$	86.64(5)	95.94(3)
$\gamma/^\circ$	77.47(7)	90
<i>V</i> /Å ³	269.7(3)	640.0(7)
<i>Z</i>	1	2
<i>D</i> _x g cm ⁻³	1.958	1.796

undergo *N*-methylation at one N-site.¹¹ The products recrystallized at isochoric conditions formed partially isostructural dimethanol solvates dabcoCH₃Br·2CH₃OH and dabcoCH₃I·2CH₃OH.

Compared to the ambient-pressure structure,²² at 0.35 GPa the unit-cell volume of 44'biPy2CH₃Br is compressed by 1.22% and the crystal exhibits a negative linear compressibility along the *a* axis, which expands, while parameters *b* and *c* shrink (Fig. 5).

The unit-cell of the 44'biPy2HBr contains one bipyridinium cation located at the inversion center, $\text{NH}^+ \cdots \text{Br}^-$ bonded to two bromide anions. Hence the pyridinium rings of the dication are parallel according to its symmetry. The next shortest contacts of the Br⁻ anions are formed to azine hydrogen atoms. The 44'biPy2HBr crystal was further compressed and its structure determined at several pressure steps

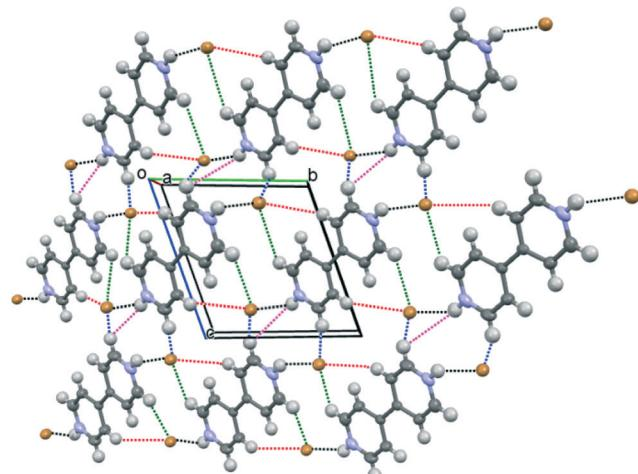


Fig. 4 Autostereogram of the crystal packing of 44'biPy2HBr viewed down the [100] direction. $\text{NH}^+ \cdots \text{Br}^-$ hydrogen bonds are marked in black, the shortest contacts $\text{CH} \cdots \text{Br}$ in dark green, blue and red and the shortest $\text{H} \cdots \text{H}$ in pink (cf. Table S4 and S5†).



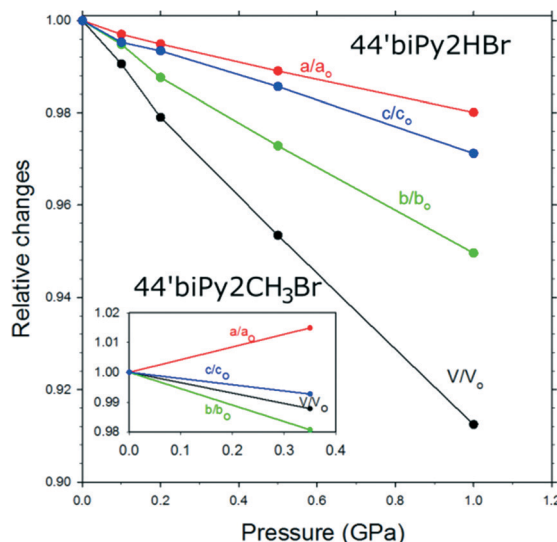


Fig. 5 Relative compression of the unit-cell dimensions of 44'biPy2HBr. The inset shows the compression of 44'biPy2CH₃Br related to the unit-cell dimensions at 0.1 MPa according to ref. 21.

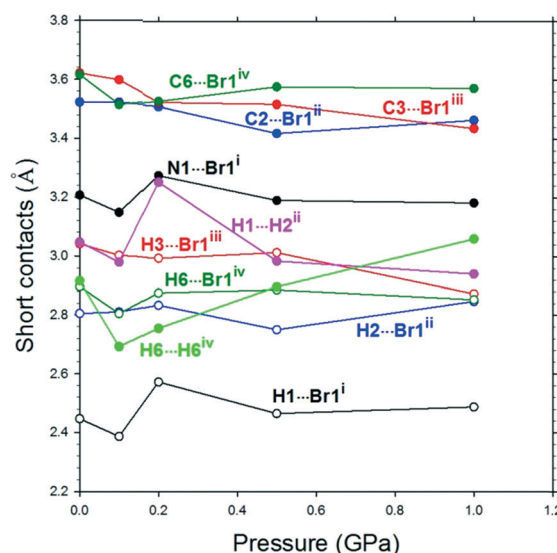


Fig. 6 The shortest contacts in 44'biPy2HBr as a function of pressure. The black lines mark the $\text{NH}^+ \cdots \text{Br}^-$ bonds, and $\text{CH} \cdots \text{Br}$ contacts are marked red, green and blue. Empty circles correspond to $\text{H} \cdots \text{H}$ contacts. The lines joining the points are for guiding the eye. The symmetry codes indicated by Roman numbers are explicitly listed in Table S4.†

up to 1.0 GPa. The compression of the unit-cell dimensions are shown in Fig. 5. In this pressure range, the $\text{NH}^+ \cdots \text{Br}^-$ bond has been squeezed from 3.207(2) to 3.184(17) Å, and the next shortest interionic contacts $\text{CH} \cdots \text{Br}$ from 3.523(3) to 3.469(43) Å (Fig. 6).

The shortest interionic interactions in 44'biPy2HBr, as expected, are $\text{NH}^+ \cdots \text{Br}^-$ hydrogen bonds and the next shortest are the $\text{C}2\text{H}_2 \cdots \text{Br}^-$, $\text{C}3\text{H}_3 \cdots \text{Br}^-$ and $\text{C}6\text{H}_6 \cdots \text{Br}^-$ contacts. The shortest contacts $\text{H} \cdots \text{H}$ are considerably longer than the sum

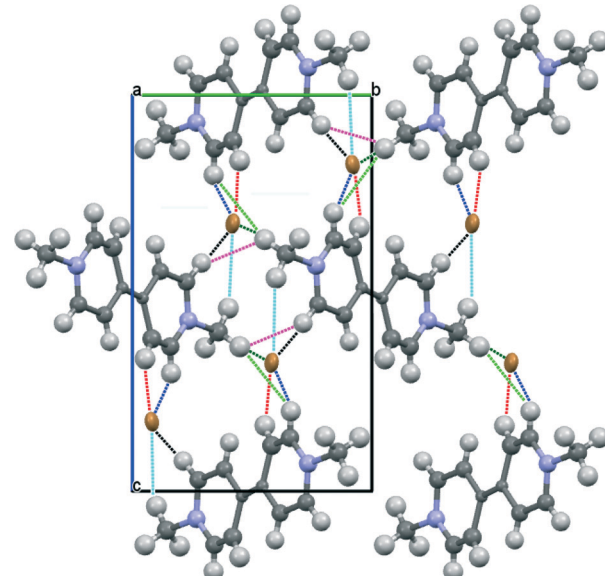


Fig. 7 Crystal packing of 44'biPy2CH₃Br at 0.35 GPa viewed down the [100] direction. The shortest contacts $\text{CH} \cdots \text{Br}$ and $\text{H} \cdots \text{H}$ are marked with blue, green, black, red and pink dotted lines (cf. Table S4.†).

of their van der Waals radii (2.4 Å according to Bondi²³). Interestingly, it appears that there is an anomalous region in the pressure dependence of intermolecular contacts at about 0.15 GPa. The $\text{NH}^+ \cdots \text{Br}^-$ bond is initially compressed and, between 0.1 and 0.2 GPa, it increases its length by over 0.2 Å. At 0.5 GPa, the $\text{NH}^+ \cdots \text{Br}^-$ bond is compressed again compared to its dimensions at 0.2 GPa; however, even at 1.0 GPa it remains longer than at 0.1 MPa and at 0.1 GPa. A similar anomalous compression occurs for the shortest $\text{CH} \cdots \text{Br}$ contacts (Fig. 6). The formation of new polymorphs at high-pressure is often related to weak hydrogen bonds.^{24,25}

Remarkably, the compressed and heated dabcoHBr does not transform to the corresponding disalt dabco₂HBr,⁷ while

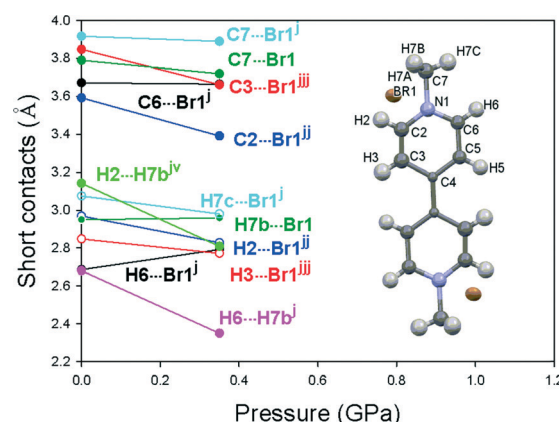


Fig. 8 The shortest contacts in 44'biPy2CH₃Br as a function of pressure (cf. Fig. 7). Empty circles correspond to $\text{H} \cdots \text{Br}$ bonds. The lines joining the points are for guiding the eye. The symmetry codes indicated by Roman numbers are explicitly listed in Table S3.† for 44'biPy2CH₃Br, letters 'j' have been used (e.g. jjj) for distinction from 44'biPy2HBr, where letter 'i' is used in the Roman numbers.

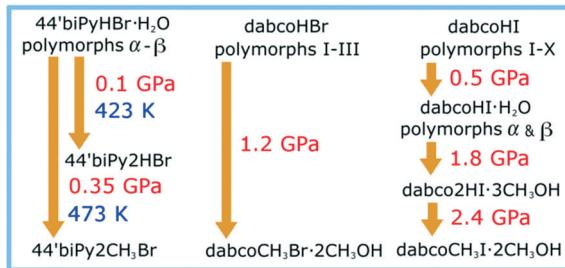


Fig. 9 Compounds precipitated from monosalts $44'\text{biPyHBr}\cdot\text{H}_2\text{O}$, dabcoHBr and dabcoHI dissolved in water and a water : methanol mixture (detailed conditions of the crystallization are described in the text).

the analogue dabcoHI at 1.8 GPa transforms to a trimethanol solvated disalt, dabco $2\text{HI}\cdot3\text{CH}_3\text{OH}$. It is likely that the *N*-methylation reaction of dabcoHBr dissolved in methanol precludes the formation of the disalt,²⁶ particularly since dabco 2HBr can be easily obtained under normal conditions from stoichiometric solutions of dabco and HBr.²¹

For the $44'\text{biPyHBr}\cdot\text{H}_2\text{O}$ sample sealed in the DAC at 0.35 GPa, then dissolved at isochoric conditions at 473 K and recrystallized by slow controlled cooling, the *N,N*-dimethylation reaction took place. The X-ray diffraction data revealed that the *N,N*-dimethylbipyridinium disalt was obtained, which implies the following reaction:



Because of the *N,N*-dimethylated dibromide disalt product, this high-pressure *N*-methylation reaction contrasts with those of dabcoHBr and dabcoHI, where mono-*N*-methylated monosalts were obtained at 1.2 and 2.4 GPa, respectively. It is plausible that the close location of the amine nitrogen atoms in dabco hampers the *N*-methylation of two ammonium groups, due to disadvantageous electrostatic interactions of their positive charges. The amine nitrogen atoms in $44'\text{biPy}$ are located 2.5 times further away compared to those in dabco, hence the Coulomb forces are over six times weaker and consequently $44'\text{biPy}$ is more prone to the double *N*-methylation. The crystal structure of $44'\text{biPy2CH}_3\text{Br}$ at high-pressure (Fig. 7) is consistent with that previously determined for this compound under normal conditions.²² The shortest contacts in this structure, $\text{CH}\cdots\text{Br}$, are all compressed except for the $\text{C}6\text{--H}6\cdots\text{Br}1^{\text{j}}$ contact (Fig. 8).

It is characteristic that in both high-pressure reactions of $44'\text{biPyHBr}\cdot\text{H}_2\text{O}$ described in this report, the unsolvated disalt products were formed and free base $44'\text{biPy}$ and H_2O were released into the solution. With respect to the preferential formation of hydrates and anhydrates, the formation of the hydrate monosalt ($44'\text{biPyHBr}\cdot\text{H}_2\text{O}$), anhydrate disalt ($44'\text{biPy2HBr}$) and *N,N*-dimethylated anhydrate ($44'\text{biPy2CH}_3\text{Br}$), these $44'\text{biPy}$ -based salts differ from their dabco analogues: anhydrate monosalt (dabcoHBr), solvated disalt and solvated mono-*N*-methylated salt, respectively, as shown in Fig. 9. Under ambient conditions,

$44'\text{biPyHBr}$ preferentially forms hydrate $44'\text{biPyHBr}\cdot\text{H}_2\text{O}$, whereas anhydrous dabcoHBr and dabcoHI are obtained from aqueous solution at 0.1 MPa. The dabco $2\text{HI}\cdot3\text{CH}_3\text{OH}$ solvate was obtained at 1.2 GPa. This different solvation can be due to the very different shape of molecules, elongated 'peanut' $44'\text{biPy}$ and bulky dabco.

Conclusion

The chemical reactions observed for $44'\text{biPyHBr}\cdot\text{H}_2\text{O}$ strongly suggest that high pressure promotes symmetric products. The symmetric dications $[44'\text{biPy2H}]^{2+}$ and $[44'\text{biPy2CH}_3]^{2+}$ can be favored by the pressure-enhanced topochemical character of the reactions, where the equivalent reaction sites 'prefer' the identical crystal environments. Compression of distances between molecules enhances their intermolecular interactions – the increase in van der Waals interactions (described by the Lennard-Jones potential $V_{\text{LJ}} = 4\epsilon[(\sigma/r)^{12} + (\sigma/r)^{-6}]$, where r is the distance, ϵ is the potential-well depth, and σ is the finite distance for $V_{\text{LJ}} = 0$) is considerably stronger depending on the distance r compared to the electrostatic potential ($V_{\text{el}} = kQq/r$, where k is Coulomb's constant and Qq are electric charges). Consequently, any difference in energy due to the crystal environment increases with pressure, and according to this energy criterion the reactions yielding symmetric products should be favored. This is indeed the case for $44'\text{biPy2HBr}$ and $44'\text{biPy2CH}_3\text{Br}$, as well as for the analogue dabco $2\text{HI}\cdot2\text{CH}_3\text{OH}$.⁸ However, the high-pressure *N*-methylation of dabcoHBr and of dabcoHI only at one site indicated that these compounds react in the solution and due to the proximity of amine groups in dabco and the positive charges of these methylated sites, the disalt formation would be hampered. The occurrence of solvated $44'\text{biPy}$ and unsolvated dabco disalts under ambient and high-pressure conditions supports the conclusion drawn above, because $44'\text{biPy}$ and dabco molecules are very different in shape and the single- or multi-component crystallization is likely to improve the space filling, essentially important at high pressure. On the other hand, high pressure also enables crystallization to be carried out at temperature considerably higher than at 0.1 MPa, which affects the molecular tumbling and the role of intermolecular interactions (H-bonds). Further studies are needed for understanding the effects of pressure and temperature and the mechanisms of high-pressure transformations and reactions of amines and their salts.

Notes and references

- 1 V. Schettino and R. Bini, Molecules under extreme conditions: Chemical reactions at high pressure, *Phys. Chem. Chem. Phys.*, 2003, 5, 1951–1965.
- 2 H. J. Mueller, Measuring the elastic properties of natural rocks and mineral assemblages under Earth's deep crustal and mantle conditions, *J. Geodyn.*, 2013, 71, 25–42.
- 3 V. L. Solozhenko and E. Gregoryanz, *Synthesis of superhard materials*, *Mater. Today*, 2005, 8, 44–51.



4 R. Mohammadi, M. Xie, A. T. Lech, C. L. Turner, A. Kavner, S. H. Tolbert and R. B. Kaner, Toward Inexpensive Superhard Materials: Tetraboride-Based Solid Solutions, *J. Am. Chem. Soc.*, 2012, **134**, 20660–20668.

5 W. Zhou, H. Wu, M. R. Hartman and T. Yildirim, Hydrogen and Methane Adsorption in Metal–Organic Frameworks: A High-pressure Volumetric Study, *J. Phys. Chem. C*, 2007, **111**, 16131–16137.

6 A. Olejniczak, A. Katrusiak and M. Szafranśki, Ten Polymorphs of $\text{NH}^+ \cdots \text{N}$ Hydrogen-Bonded 1,4-Diazabicyclo[2.2.2]octane Complexes: Supramolecular Origin of Giant Anisotropic Dielectric Response in Polymorph, *Cryst. Growth Des.*, 2010, **10**, 3537–3546.

7 W. Nowicki, A. Olejniczak, M. Andrzejewski and A. Katrusiak, Reverse sequence of transitions in prototypic relaxor 1,4-diazabicyclo[2.2.2]octane, *CrystEngComm*, 2012, **14**, 6428–6434.

8 A. Olejniczak and A. Katrusiak, Pressure-Induced Hydration of 1,4-Diazabicyclo[2.2.2]octane Hydroiodide (dabcoHI), *Cryst. Growth Des.*, 2011, **11**, 2250–2256.

9 A. Olejniczak, M. Podsiadło and A. Katrusiak, High pressure used for producing a new solvate of 1,4-diazabicyclo[2.2.2]octane hydroiodide, *New J. Chem.*, 2016, **40**, 2014–2020.

10 A. Olejniczak and A. Katrusiak, Pressure induced transformations of 1,4-diazabicyclo[2.2.2]octane (dabco) hydroiodide diprotonation of dabco, its *N*-methylation and co-crystallization with methanol, *CrystEngComm*, 2010, **12**, 2528–2532.

11 M. Andrzejewski, A. Olejniczak and A. Katrusiak, Remote halogen switch of amine hydrophilicity, *CrystEngComm*, 2012, **14**, 6374–6376.

12 M. Anioła and A. Katrusiak, Conformational conversion of 4,4'-bipyridinium in a hidden high-pressure phase, *Cryst. Growth Des.*, 2015, **14**, 2187–2191.

13 F. H. Allen, The Cambridge Structural Database: A Quarter of a Million Crystal Structures and Rising, *Acta Crystallogr., Sect. B: Struct. Sci.*, 2002, **58**, 380–388.

14 L. Merrill and W. A. Bassett, Miniature diamond anvil pressure cell for single crystal X-ray diffraction studies, *Rev. Sci. Instrum.*, 1974, **45**, 290.

15 A. Katrusiak, High-pressure crystallography, *Acta Crystallogr., Sect. A: Found. Crystallogr.*, 2008, **64**, 135–148.

16 G. J. Piermarini, S. Block, J. D. Barnett and R. A. Forman, Calibration of the pressure dependence of the R1 ruby fluorescence line to 195 kbar, *J. Appl. Phys.*, 1975, **46**, 2774–2780.

17 H. K. Mao, J. Xu and P. M. Bell, Calibration of the ruby pressure gauge to 800 kbar under quasi-hydrostatic conditions, *J. Geophys. Res., B*, 1985, **91**, 4673–4676.

18 Xcalibur CCD System, *CrysAlisPro Software System, version 1.171.33*, Oxford Diffraction Ltd.: Oxfordshire, U.K., 2004.

19 A. Katrusiak, REDSHABS, *Program for the correcting reflections intensities for DAC absorption, gasket shadowing and sample crystal absorption*, Adam Mickiewicz University, Poznań, Poland, 2003.

20 B. S. Zhang and Y. Q. Zheng, Crystal structure of 4,4'-bipyridinium dibromide ($\text{C}_{10}\text{H}_{10}\text{N}_2\text{Br}_2$), *Z. Kristallogr. NCS*, 2003, **218**, 421–422.

21 M. Andrzejewski, A. Olejniczak and A. Katrusiak, Humidity Control of Isostructural Dehydration and Pressure-Induced Polymorphism in 1,4-Diazabicyclo[2.2.2]octane Dihydrobromide Monohydrate, *Cryst. Growth Des.*, 2011, **11**, 4892–4899.

22 J. H. Russell and S. C. Wallwork, The Crystal Structure of the Dichloride and Isomorphous Dibromide and Diiodide of the *N,N*'-Dimethyl-4,4'-bipyridinium Ion, *Acta Crystallogr., Sect. B: Struct. Crystallogr. Cryst. Chem.*, 1972, **28**, 1527.

23 A. Bondi, Van der Waals Volume and Radii, *J. Phys. Chem.*, 1964, **68**, 441–451.

24 E. V. Boldyreva, High-pressure studies of the hydrogen bond networks in molecular crystals, *J. Mol. Struct.*, 2004, **700**, 151–155.

25 F. P. A. Fabbiani, D. R. Allan, W. I. F. David, S. M. Moggach, S. Parsons and C. R. Pulham, High-pressure recrystallization – a route of new polymorphs and solvates, *CrystEngComm*, 2004, **6**, 504–511.

26 A. Budzianowski and A. Katrusiak, Pressure Tuning between $\text{NH} \cdots \text{N}$ Hydrogen-Bonded Ice Analogue and $\text{NH} \cdots \text{Br}$ Polar dabcoHBr Complexes, *J. Phys. Chem. B*, 2006, **110**, 9755–9758.

